Advanced sections

Modeling complex sections in SectionPro

Application to a prestressed bridge box-girder section over a support

BridgeKernel · 2026

Introduction

Standard beam, column and wall sections are generally described by a single contour and uniform reinforcement. Real structures often combine several materials, voids, separate reinforcement layers, prestressing tendons or embedded steel members. Their analysis requires a representation that preserves both the geometry and the constitutive law of every component.

SectionPro advanced sections address this need. An advanced section is assembled from geometric domains, passive reinforcement, prestressing steel, structural steel sections and thin plates. Each component is assigned the material law used by the analyses. The same description is then used to calculate section properties, verify stresses and strains under applied section forces, calculate crack widths and generate interaction domains.

This article first presents the data model of an advanced section. A critical section over a support in a prestressed concrete box girder is then used as an example. This geometry combines a large void, reinforcement distributed along several faces and groups of tendons within one model.

Defining an advanced section

An advanced section combines several families of mechanical objects. The solver preserves their position in the section coordinate system and evaluates their contribution using the law assigned to each object.

- A geometric domain, or GeoDomain, is defined by an outer contour and may contain several voids. One section may contain several domains, each with its own material law.
- Passive reinforcement is organised into independent layers. Each bar has a position, a diameter and a steel law, allowing separate layers, faces and steel grades to be represented.
- Prestressing steel is grouped into tendon families defined by their positions, areas, bond parameters and initial state.
- Structural steel sections can be selected from the integrated library of 535 profiles covering eleven European families: IPE, HEA, HEB, HEM, UNP, UPE, UAP, LNP, and square, rectangular and

circular hollow sections. They may be represented either by a GeoDomain integrated over the actual area, including curved transitions and fillets, or by an assembly of TSP elements.

- A TSP element describes the straight or curved midline of a plate and its thickness. Its contribution is obtained by line integration, with stress assumed uniform through the thickness. This representation is suited to thin plates, structural steel sections and multicell box sections.
- Material laws are assigned directly to the components. They may use the code-based models provided by SectionPro or a general user-defined stress–strain relationship for the limit states under consideration.

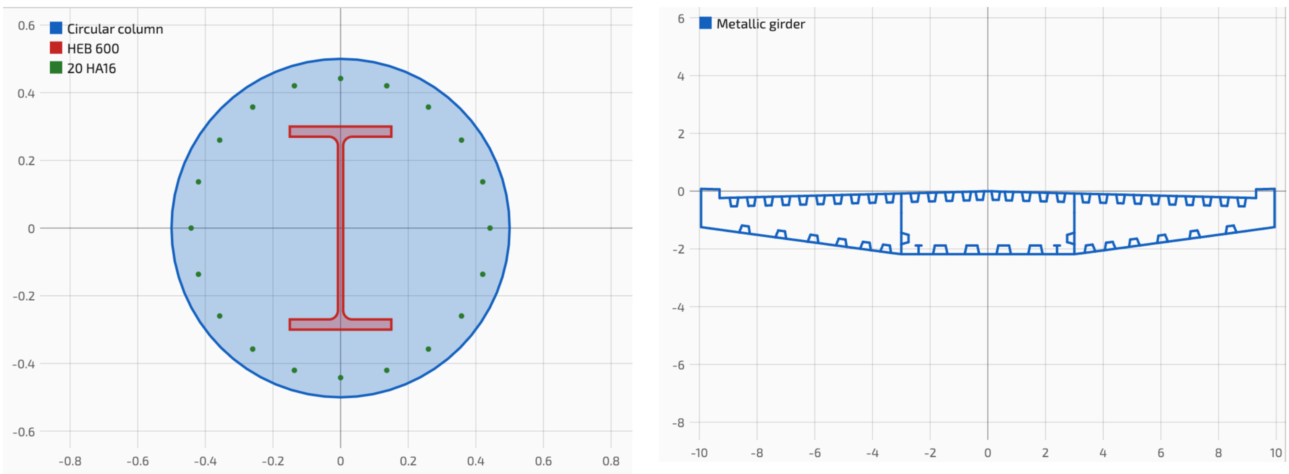

Composite column: concrete, HEB section and passive reinforcement.

Steel box girder: 267 TSP elements and 51 Bredt cells.

Figure 1: Examples of advanced sections displayed in SectionPro.

Example: bridge box girder

The section studied is a critical section over a support in a single-cell box girder. It is 12.00 m wide and 2.70 m deep. The top slab, inclined webs, haunches and bottom slab form a single concrete domain. The central cell is defined as an internal void.

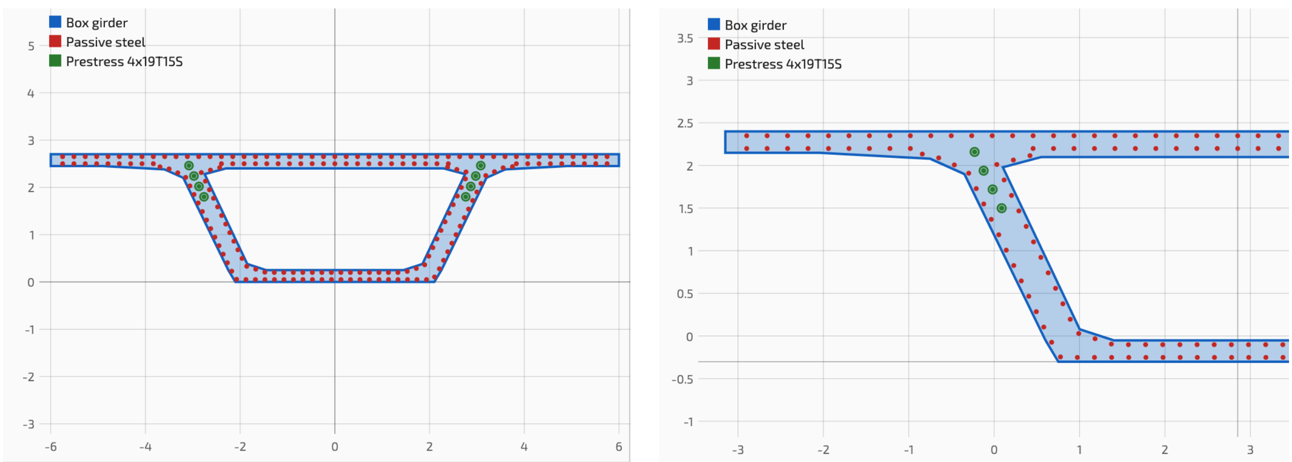

(a) Overall view of the section.

(b) Detail of the upper left gusset.

Figure 2: SectionPro model: concrete domain, passive reinforcement and prestressing groups.

Component	Material	Definition in example
GeoDomain 1	Concrete C45/55	Contour of the box, one interior cell, gross area of 6,759 m^2
Passive reinforcement	B500B	186 HA16 bars distributed 50 mm from the concrete faces
Prestressing	Y1860	Eight 19T15S tendons, four along each web, an area of 2,850 mm^2 per tendon and 100 mm ducts

The section contains 186 reinforcing bars and eight prestressing tendons. The four ducts along each web are aligned with the web direction and extend into the upper haunch. Their coordinates are generated by script and then saved in the advanced-section file. The same file is used for all analyses presented below.

Section forces and prestressing

The total section-force vector is decomposed into the effects of permanent loads G, variable loads Q and prestressing P: $\boldsymbol{S} = \boldsymbol{S}_G + \boldsymbol{S}_Q + \boldsymbol{S}_P$.

For the section considered, the finite-element structural model developed in our LFEM software gives the following $G+Q$ section-force vectors, in MN and MN $\cdot$ m: $\boldsymbol{S}_{G+Q}^{\mathrm{SLS}} = (0; -58,650; 0)$ and $\boldsymbol{S}_{G+Q}^{\mathrm{ULS}} = (0; -92,650; 0)$.

In SectionPro, prestressing is considered at two levels. Its action on the structure, including the primary effect and any secondary effect, must be included in the applied section-force vector. The transverse symmetry of the section and tendon profile gives no moment about y here; therefore $\boldsymbol{S}_P = \left(N_P, M_{z,P}^{\mathrm{primary}} + M_{z,P}^{\mathrm{secondary}}, 0\right)$.

The effective tendon stress defines the initial state associated with the prestressing action. In the resistance calculation, the equilibrium strain state then changes the tendon stress: elongation produces a positive stress increment and increases the tendon contribution, whereas shortening produces a stress decrease.

In the example, the effective stress after losses is 1116 MPa. The corresponding action produces an axial force of 25.445 MN. At the support section, the tendons lie above the centroid, giving a primary moment of $+8,994$ MN $\cdot$ m. For this tendon profile, the structural model gives a secondary moment of the same sign, equal to $+4,400$ MN $\cdot$ m. The prestressing moment introduced in the section is therefore $+13,394$ MN $\cdot$ m.

Final section-force vector	N [MN]	M_z [MN·m]	M_y [MN·m]
SLS	25,445	$-45,256$	0,000
ULS	25,445	$-79,256$	0,000

Results on the full model

Mechanical characteristics

SectionPro calculates the properties of the gross, net and transformed sections. In this example, only the prestressing ducts are deducted from the net section; the passive reinforcement is retained. In the transformed section, both passive and prestressing steel use the modular ratio $n = 5$.

Section	A [m²]	y_G [m]	I_{zz} [m⁴]	I_{yy} [m⁴]
Gross	6,7590	1,7765	6,4096	55,5258
Net	6,6962	1,7732	6,3979	54,9883
Homogenized	6,9598	1,7777	6,5809	57,1632

The torsion and shear properties of the gross section are given below.

J [m⁴]	A_{sy} [m²]	A_{sz} [m²]	y_T [m]	Γ [m⁶]
13,6059	1,5031	4,5502	1,3508	6,5277

The field shown below corresponds to the shear stresses produced by a unit torque.

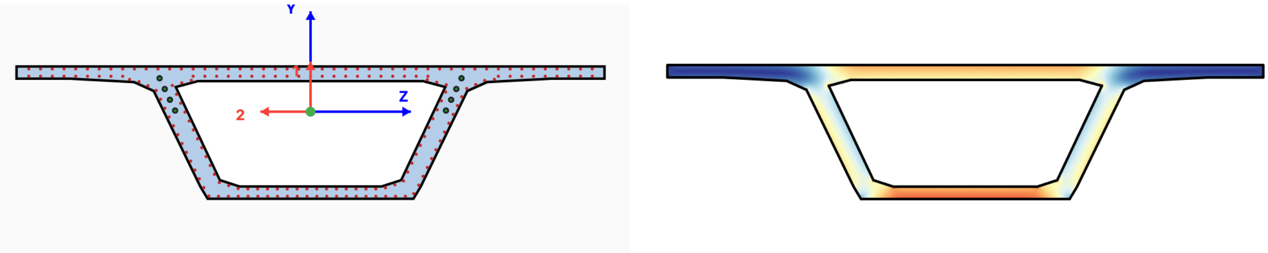

Figure 3: Centroidal and principal axes (left), and shear-stress field under unit torsion (right).

Equilibrium at the SLS and ULS

The solver determines the section strain state that equilibrates the applied section forces. Stresses are then obtained from the respective constitutive laws of concrete, passive reinforcement and tendons. The results presented correspond to the characteristic SLS combination and the fundamental ULS combination.

For tendons, the final stress is evaluated from the cumulative strain $\varepsilon_0 + \Delta\varepsilon_1 + \Delta\varepsilon_2$. The term ε_0 is the strain associated with the effective stress of 1116 MPa; $\Delta\varepsilon_1$ represents any decompression of the concrete adjacent to the tendon; and $\Delta\varepsilon_2$ is the strain obtained from section equilibrium. The decompression effect is enabled in this example.

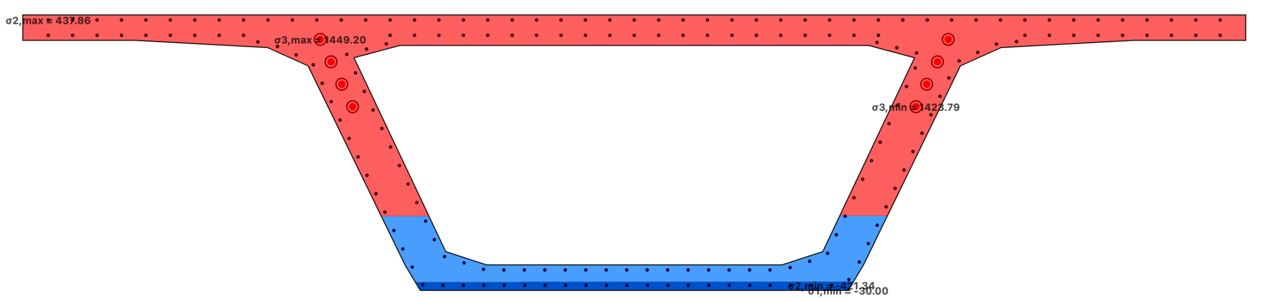

Figure 4: ULS normal-stress field obtained from the nonlinear verification of the final section-force vector.

Result	Unit	Characteristic SLS	Fundamental ULS
Concrete			
Minimum strain, $\varepsilon_{b,\mathrm{min}}$	‰	$-0,531$	$-2,262$
Minimum stress, $\sigma_{b,\mathrm{min}}$	MPa	$-19,264$	$-30,000$
Passive steels			
Minimum strain, $\varepsilon_{s,\mathrm{min}}$	‰	$-0,512$	$-2,107$
Maximum strain, $\varepsilon_{s,\mathrm{max}}$	‰	0,495	5,946
Minimum stress, $\sigma_{s,\mathrm{min}}$	MPa	$-102,31$	$-421,34$
Maximum stress, $\sigma_{s,\mathrm{max}}$	MPa	99,09	437,86
Prestressing			
Minimum strain, $\varepsilon_{p,\mathrm{min}}$	‰	0,166	3,297
Minimum total stress, $\sigma_{p,\mathrm{min}}$	MPa	1148,32	1423,79
Minimum stress increment, $\Delta\sigma_{p,\mathrm{min}}$	MPa	32,32	307,79
Maximum strain, $\varepsilon_{p,\mathrm{max}}$	‰	0,422	5,352
Maximum total stress, $\sigma_{p,\mathrm{max}}$	MPa	1198,23	1449,20
Maximum stress increment, $\Delta\sigma_{p,\mathrm{max}}$	MPa	82,23	333,20
Resolution			
Iterations		4	6
Convergence residual		$1,0 \times 10^{-11}$	$4,7 \times 10^{-7}$
Convergence		Yes	Yes

At the fundamental ULS, the bottom-slab concrete locally reaches its plastic compression plateau, while a substantial tensile zone develops in the top slab and upper parts of the webs. The tendons are strongly mobilised, with stress increments between 307.8 and 333.2 MPa.

At the characteristic SLS, the stress checks are satisfied: the maximum concrete compressive stress is 19.264 MPa, the maximum tensile stress in the passive reinforcement is 99.09 MPa and the maximum total tendon stress is 1198.23 MPa. The crack width, $w_k = 0,174$ mm, remains small even though it is evaluated here under the characteristic combination.

Interaction domains

The advanced geometry and material laws are also used to calculate resistance domains. The N-M_z curve is a slice through the domain at $M_y = 0$. The N-M_z-M_y surface extends the calculation to every bending direction.

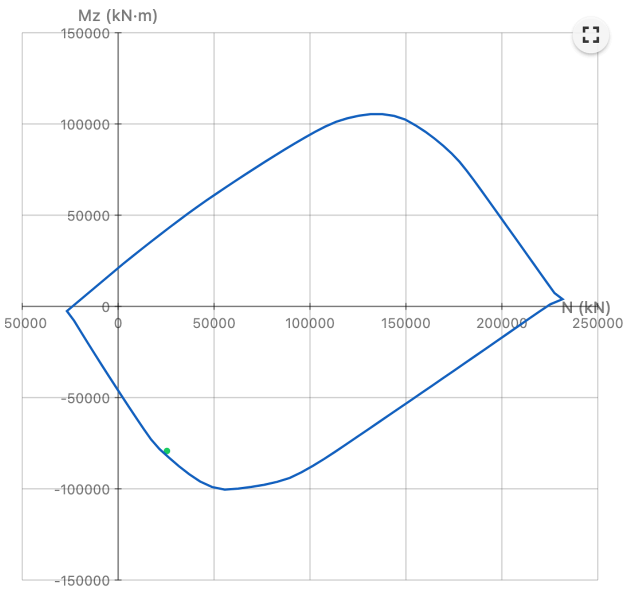

Figure 5: N-M_z interaction curve at the ULS for $M_y = 0$, with the final section-force vector shown.

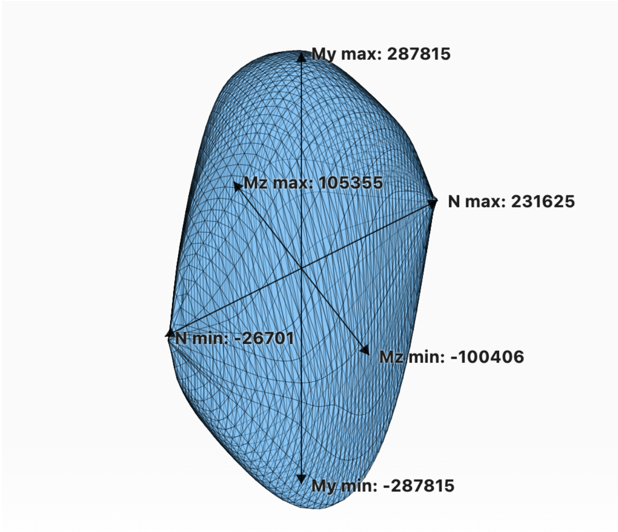

Figure 6: N-M_z-M_y interaction surface at the ULS.

The following table gives the bounding box of the interaction surface, defined by the minimum and maximum values of each of its three components.

Component	Minimum	Maximum
N	$-26,70$ MN	231.62 MN
M_z	$-100,41$ MN · m	105.35 MN · m
M_y	$-287,82$ MN · m	287.82 MN · m

The positive and negative capacities about M_y coincide, as expected from the transverse symmetry of the section. The difference between the positive and negative capacities about M_z reflects the different geometry and reinforcement of the top and bottom slabs. The final section-force vector lies very close to the boundary of the resistance domain. The distance-to-domain module gives $FS = 0,983$: slightly below unity, but very close to the limit.

Performance

The table below shows the execution times of calls to the SectionPro kernel on the box model. These values exclude the GUI and rendering of results.

Analysis	Calculation time
Mechanical characteristics	28.3 ms
State of stresses and strains	0.73 ms
Crack opening calculation	2.38 ms
N-M_z interaction curve, 200 points	1.11 ms
Interaction surface N-M_z-M_y, mesh 50 × 50	208 ms

These results illustrate one of SectionPro's strengths: extensive kernel optimisation keeps computation times extremely low, including for nonlinear analyses and the construction of three-dimensional resistance domains. Checks and design iterations therefore return almost immediately, which directly contributes to a fluid user experience.

Conclusion

Advanced sections combine several geometric domains and their voids, layers of passive reinforcement, groups of prestressing steel, structural steel sections and thin plates within a single model. Each component retains its own material law at the different limit states.

The box girder studied here illustrates this representation. Its support section combines a voided concrete domain, reinforcement distributed along the faces and prestressing tendons following the webs. Prestressing enters the applied section-force vector through its primary and secondary effects. The tendon contribution to resistance is evaluated from the change in tendon stress, taking account of the initial prestress, any decompression of the adjacent concrete and the equilibrium strain state of the section.

Advanced mode can therefore analyse virtually any cross-section, regardless of geometric complexity or the materials from which it is assembled. This generality naturally remains subject to the assumptions of cross-section analysis, in particular that plane sections remain plane and that linked components satisfy strain compatibility. Thanks to the optimised calculation kernel, even these detailed models retain near-instantaneous response times.